

Structure of $A = 10 - 13$ nuclei with two- plus three-nucleon interactions from chiral effective field theory

P. Navrátil,¹ V. G. Gueorguiev,¹ J. P. Vary,^{1,2} W. E. Ormand,¹ and A. Nogga³

¹Lawrence Livermore National Laboratory, P.O. Box 808, L-414, Livermore, CA 94551, USA

²Department of Physics and Astronomy, Iowa State University, Ames, Iowa 50011, USA

³Forschungszentrum Jülich, Institut für Kernphysik (Theorie), D-52425 Jülich, Germany

(Dated: August 5, 2021)

Properties of finite nuclei are evaluated with two-nucleon (NN) and three-nucleon (NNN) interactions derived within chiral effective field theory (EFT). The nuclear Hamiltonian is fixed by properties of the $A = 2$ system, except for two low-energy constants (LECs) that parameterize the short range NNN interaction. We constrain those two LECs by a fit to the $A = 3$ system binding energy and investigate sensitivity of ${}^4\text{He}$, ${}^6\text{Li}$, ${}^{10,11}\text{B}$ and ${}^{12,13}\text{C}$ properties to the variation of the constrained LECs. We identify a preferred choice that gives globally the best description. We demonstrate that the NNN interaction terms significantly improve the binding energies and spectra of mid- p -shell nuclei not just with the preferred choice of the LECs but even within a wide range of the constrained LECs. At the same time, we find that a very high quality description of these nuclei requires further improvements to the chiral Hamiltonian.

PACS numbers: 21.60.Cs, 21.30.-x, 21.30.Fe, 27.20.+n

The nuclear strong interaction has proven to be complicated and replete with ambiguities. However, chiral perturbation theory (ChPT) [1] provides a promising bridge to the underlying theory, QCD, that could remove ambiguities. Beginning with the pionic or the nucleon-pion system [2] one works consistently with systems of increasing nucleon number [3, 4, 5]. One makes use of spontaneous breaking of chiral symmetry to systematically expand the strong interaction in terms of a generic small momentum and takes the explicit breaking of chiral symmetry into account by expanding in the pion mass. Thereby, the NN interaction, the NNN interaction and also πN scattering are related to each other. At the same time, the pion mass dependence of the interaction is known, which will enable a connection to lattice QCD calculations in the future [6]. Nuclear interactions are non-perturbative, because diagrams with purely nucleonic intermediate states are enhanced [1]. Therefore, the ChPT expansion is performed for the potential. Solving the Schrödinger equation for this potential then automatically sums diagrams with purely nucleonic intermediate states to all orders. Up to the fourth- or next-to-next-to-next-to-leading order (N^3LO) of the ChPT, all the LECs can be determined by the $A = 2$ data with the exception of two LECs that must be fitted to properties of $A > 2$ systems. The resulting Hamiltonian predicts all other nuclear properties, including those of heavier nuclei. We demonstrate that this reductive program works to predict the properties on mid- p -shell nuclei with increasing accuracy when the NNN interaction is included.

We adopt the potentials of ChPT at the orders presently available, the NN at N^3LO of Ref. [7] and the NNN interaction at N^2LO [8]. Since the NN interaction is non-local, the *ab initio* no-core shell model (NCSM) [9, 10, 11] is the only approach currently available to

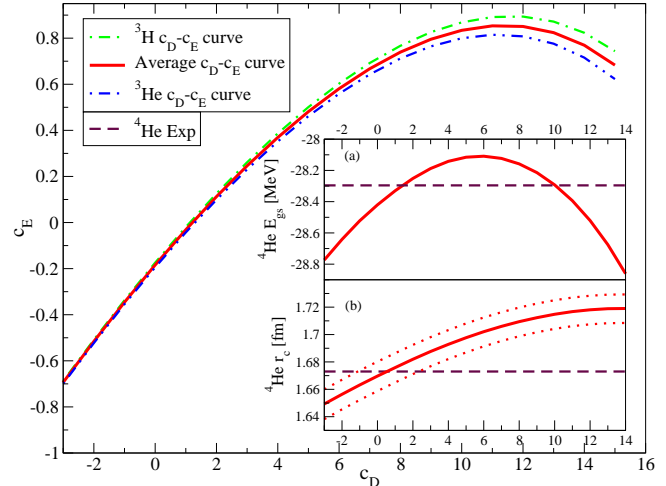


FIG. 1: Relations between c_D and c_E for which the binding energy of ${}^3\text{H}$ (8.482 MeV) and ${}^3\text{He}$ (7.718 MeV) are reproduced. (a) ${}^4\text{He}$ ground-state energy along the averaged curve. (b) ${}^4\text{He}$ charge radius r_c along the averaged curve. Dotted lines represent the r_c uncertainty due to the uncertainties in the proton charge radius.

solve the resulting many-body Schrödinger equation for mid- p -shell nuclei. In this paper, we use the NCSM to evaluate binding energies, spectra and other observables for ${}^6\text{Li}$, ${}^{10,11}\text{B}$ and ${}^{12,13}\text{C}$. We also present our results for the s -shell nuclei ${}^3\text{H}$, ${}^3\text{He}$ and ${}^4\text{He}$. We use the $A = 3$ binding energies to constrain the two unknown LECs of the NNN contact terms, c_D and c_E [12]. We then investigate sensitivity of the $A > 3$ nuclei properties to the variation of the constrained LECs. Our approach differs in two aspects from the first NCSM application of the chiral NN+NNN interactions in Ref. [12] which presents a detailed investigation of ${}^7\text{Li}$. First, we introduce a reg-

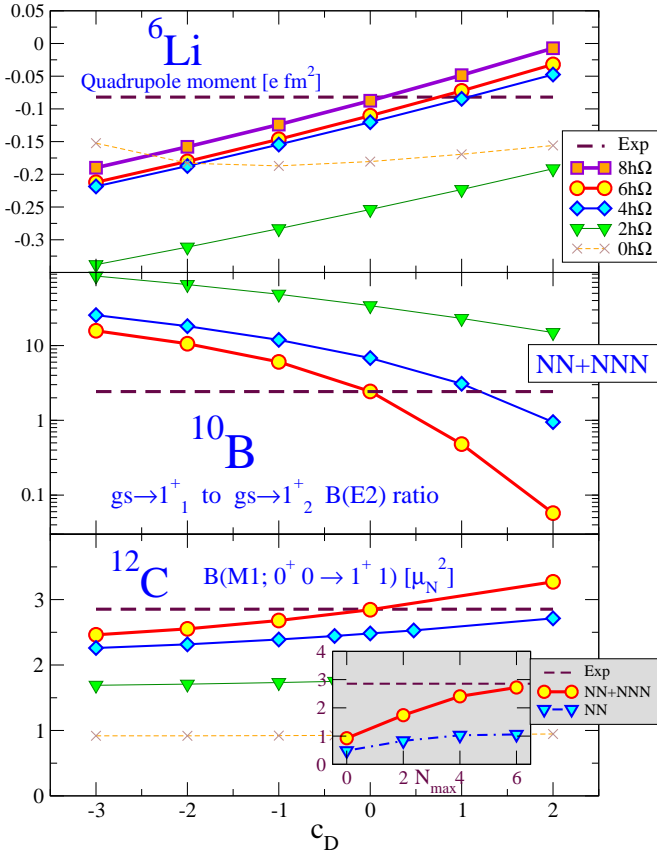


FIG. 2: Dependence on the c_D with the c_E constrained by the $A = 3$ binding energy fit for different basis sizes for: ^6Li quadrupole moment, ^{10}B $B(\text{E}2; 3_1^+ 0 \rightarrow 1_1^+ 0) / B(\text{E}2; 3_1^+ 0 \rightarrow 1_2^+ 0)$ ratio, and the ^{12}C $B(\text{M}1; 0^+ 0 \rightarrow 1^+ 1)$. The HO frequency of $\hbar\Omega = 13, 14, 15$ MeV was employed for ^6Li , ^{10}B , ^{12}C , respectively. In the inset of the ^{12}C figure, the convergence of the $B(\text{M}1; 0^+ 0 \rightarrow 1^+ 1)$ is presented for calculations with (using $c_D = -1$) and without the NNN interaction.

ulator depending on the momentum transfer in the NNN terms which results in a local chiral NNN interaction. Second, we do not use exclusively the ^4He binding energy as the second constraint on the c_D and c_E LECs.

The NCSM casts the diagonalization of the infinite dimensional many-body Hamiltonian matrix as a finite matrix problem in a harmonic oscillator (HO) basis with an equivalent “effective Hamiltonian” derived from the original Hamiltonian. The finite matrix problem is defined by N_{\max} , the maximum number of oscillator quanta shared by all nucleons above the lowest configuration. We solve for the effective Hamiltonian by approximating it as a 3-body interaction [10, 11] based on our chosen chiral NN+NNN interaction. With this “cluster approximation”, convergence is guaranteed with increasing N_{\max} .

It is important to note that our NCSM results through $A = 4$ are fully converged in that they are independent of the cutoff, N_{\max} , and the HO energy, $\hbar\Omega$. For heavier

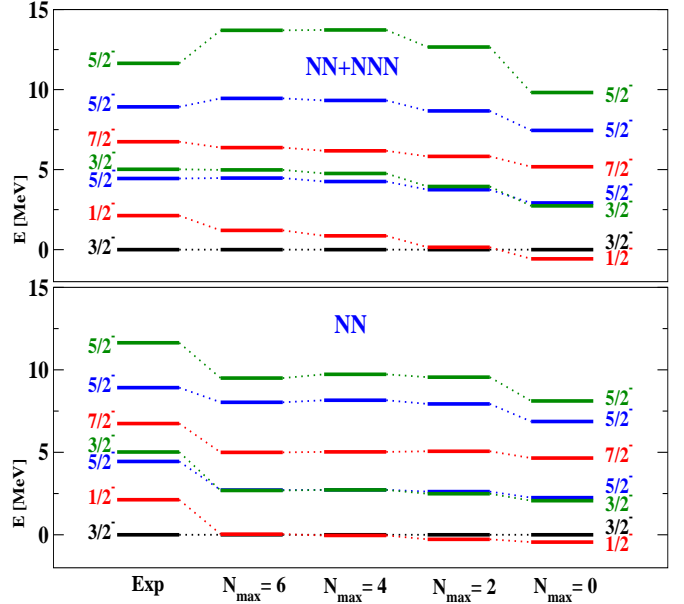


FIG. 3: ^{11}B excitation spectra as function of the basis space size N_{\max} at $\hbar\Omega = 15$ MeV and comparison with experiment. The isospin of the states depicted is $T=1/2$.

systems, we characterize the approach to convergence by the dependence of results on N_{\max} and $\hbar\Omega$.

Fig. 1 shows the trajectories of the two LECs $c_D - c_E$ that are determined from fitting the binding energies of the $A = 3$ systems. Separate curves are shown for ^3H and ^3He fits, as well as their average. There are two points where the binding of ^4He is reproduced exactly. We observe, however, that in the whole investigated range of $c_D - c_E$, the calculated ^4He binding energy is within a few hundred keV of experiment. Consequently, the determination of the LECs in this way is likely not very stringent. We therefore investigate the sensitivity of the p -shell nuclear properties to the choice of the $c_D - c_E$ LECs. First, we maintain the $A = 3$ binding energy constraint. Second, we limit ourselves to the c_D values in the vicinity of the point $c_D \sim 1$ since the values close to the point $c_D \sim 10$ overestimate the ^4He radius.

While most of the p -shell nuclear properties, e.g. excitation spectra, are not very sensitive to variations of c_D in the range from -3 to +2 that we explored, we identified several observables that do demonstrate strong dependence on c_D . In Fig. 2 we display the ^6Li quadrupole moment that changes sign depending on the choice of c_D , the ratio of the $B(\text{E}2)$ transitions from the ^{10}B ground state to the first and the second $1^+ 0$ state, and the ^{12}C $B(\text{M}1)$ transition from the ground state to the $1^+ 1$ state. The $B(\text{M}1)$ transition inset illustrates the importance of the NNN interaction in reproducing the experimental value [13]. The ^{10}B $B(\text{E}2)$ ratio in particular changes by several orders of magnitude depending on the c_D variation. This is due to the fact that the structure of the

two 1^+0 states is exchanged depending on c_D . Using extrapolation, we can see that the best overall description is obtained around the $c_D \approx -1$. This observation is also supported by excitation energy calculations as well as by calculations of other transitions. We therefore select $c_D = -1$ and, from Fig. 1, $c_E = -0.346$ for our further investigation.

We present in Fig. 3 the excitation spectra of ^{11}B as a function of N_{max} for both the chiral NN+NNN, (top panel) as well as with the chiral NN interaction alone (bottom panel). In both cases, the convergence with increasing N_{max} is quite good especially for the lowest-lying states. Similar convergence rates are obtained for our other p -shell nuclei.

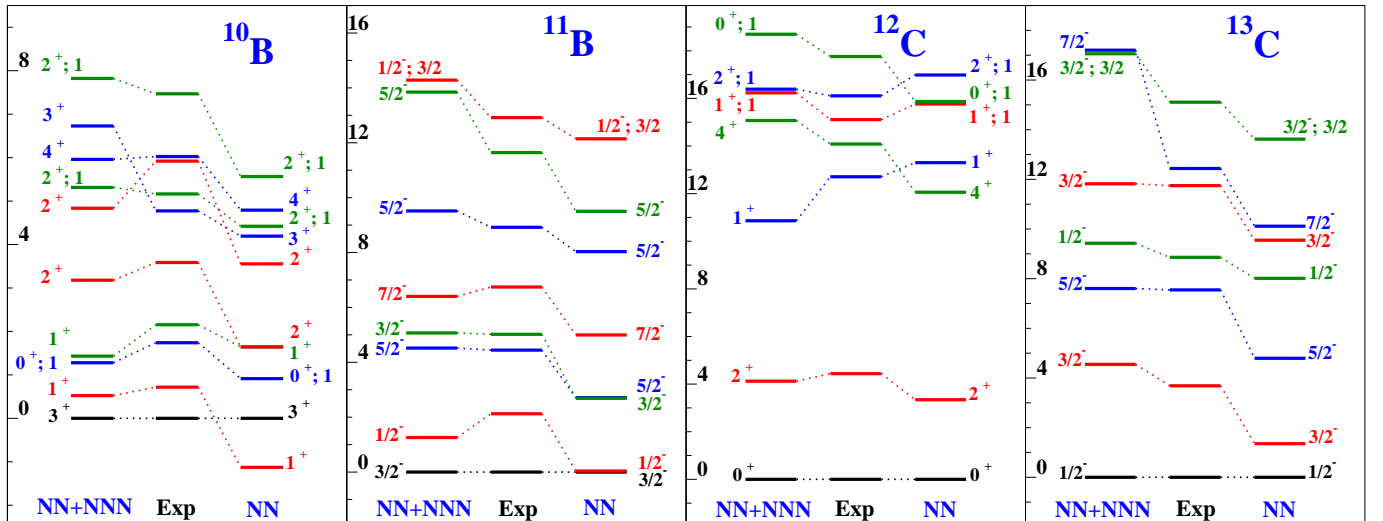


FIG. 4: States dominated by p -shell configurations for ^{10}B , ^{11}B , ^{12}C , and ^{13}C calculated at $N_{\text{max}} = 6$ using $\hbar\Omega = 15$ MeV (14 MeV for ^{10}B). Most of the eigenstates are isospin $T=0$ or $1/2$, the isospin label is explicitly shown only for states with $T=1$ or $3/2$. The excitation energy scales are in MeV.

We display in Fig. 4 the natural parity excitation spectra of four nuclei in the middle of the p -shell with both the NN and the NN+NNN effective interactions from ChPT. The results shown are obtained in the largest basis spaces achieved to date for these nuclei with the NNN interactions, $N_{\text{max}} = 6$ ($6\hbar\Omega$). Overall, the NNN interaction contributes significantly to improve theory in comparison with experiment. This is especially well-demonstrated in the odd mass nuclei for the lowest few excited states. The celebrated case of the ground state spin of ^{10}B and its sensitivity to the presence of the NNN interaction is clearly evident. There is an initial indication in these spectra that the chiral NNN interaction is “over-correcting” the inadequacies of the NN interaction since, e.g. 1^+0 and the 4^+0 states in ^{12}C are not only interchanged but they are also spread apart more than the experimentally observed separation. While these results display a favorable trend with the addition of NNN interaction, there is room for additional improvement and we discuss the possibilities below.

These results required substantial computer resources. A typical $N_{\text{max}} = 6$ spectrum shown in Fig. 4 and a

set of additional experimental observables, takes 4 hours on 3500 processors of the LLNL’s Thunder machine. We present only an illustrative subset of our results here.

Table I contains selected experimental and theoretical results for ^6Li and $A = 10 - 13$. A total of 71 experimental data are summarized in this table including the excitation energies of 28 states encapsulated in the rms energy deviations. Note that the only case of an increase in the rms energy deviation with inclusion of NNN interaction is ^{13}C and it arises due to the upward shift of the $\frac{7}{2}^-$ state seen in Fig. 4, an indication of an overly strong correction arising from the chiral NNN interaction. However, the experimental $\frac{7}{2}^-$ may have significant intruder components and is not well-matched with our state.

We demonstrated here that the chiral NNN interaction makes substantial contributions to improving the spectra and other observables. However, there is room for further improvement in comparison with experiment. We stress that we used a strength of the 2π -exchange piece of the NNN interaction, which is consistent with the NN interaction that we employed. Since this strength is some-

TABLE I: Selected properties of ${}^6\text{Li}$, ${}^{10,11}\text{B}$ and ${}^{12,13}\text{C}$ from experiment and theory. E2 transitions are in $e^2 \text{ fm}^4$ and M1 transitions are in μ_N^2 . The rms deviations of excited state energies are quoted for the states shown in Fig. 4 whose spin-parity assignments are well established and that are known to be dominated by p -shell configurations. The total energy rms is for the 28 excited states from Fig. 4. Results were obtained in the basis spaces with $N_{\max} = 6$ (8 for ${}^6\text{Li}$) and HO frequency $\hbar\Omega = 15$ MeV (13 MeV for ${}^6\text{Li}$, 14 MeV for ${}^{10}\text{B}$). The experimental values are from Ref. [14, 15, 16, 17, 18, 19, 20, 21].

Nucleus/property	Expt.	NN+NNN	NN
${}^6\text{Li} : E(1_1^{\pm}0) [\text{MeV}]$	31.995	32.63	28.98
$Q(1_1^{\pm}0) [e \text{ fm}^2]$	-0.082(2)	-0.124	-0.052
$\mu(1_1^{\pm}0) [\mu_N]$	+0.822	+0.836	+0.845
$E_x(3_1^{\pm}0) [\text{MeV}]$	2.186	2.471	2.874
$B(\text{E2};3_1^{\pm}0 \rightarrow 1_1^{\pm}0)$	10.69(84)	3.685	4.512
$B(\text{E2};2_1^{\pm}0 \rightarrow 1_1^{\pm}0)$	4.40(2.27)	3.847	4.624
$B(\text{M1};0_1^{\pm}1 \rightarrow 1_1^{\pm}0)$	15.43(32)	15.038	15.089
$B(\text{M1};2_1^{\pm}1 \rightarrow 1_1^{\pm}0)$	0.149(27)	0.075	0.031
${}^{10}\text{B} : E(3_1^{\pm}0) [\text{MeV}]$	64.751	64.78	56.11
$r_p [\text{fm}]$	2.30(12)	2.197	2.256
$Q(3_1^{\pm}0) [e \text{ fm}^2]$	+8.472(56)	+6.327	+6.803
$\mu(3_1^{\pm}0) [\mu_N]$	+1.801	+1.837	+1.853
$rms(\text{Exp} - \text{Th}) [\text{MeV}]$	-	0.823	1.482
$B(\text{E2};1_1^{\pm}0 \rightarrow 3_1^{\pm}0)$	4.13(6)	3.047	4.380
$B(\text{E2};1_1^{\pm}0 \rightarrow 3_1^{\pm}0)$	1.71(0.26)	0.504	0.082
$B(\text{GT};3_1^{\pm}0 \rightarrow 2_1^{\pm}1)$	0.083(3)	0.070	0.102
$B(\text{GT};3_1^{\pm}0 \rightarrow 2_1^{\pm}1)$	0.95(13)	1.222	1.487
${}^{11}\text{B} : E(\frac{3}{2}_1^{\pm}\frac{1}{2}) [\text{MeV}]$	76.205	77.52	67.29
$r_p(\frac{3}{2}_1^{\pm}\frac{1}{2}) [\text{fm}]$	2.24(12)	2.127	2.196
$Q(\frac{3}{2}_1^{\pm}\frac{1}{2}) [e \text{ fm}^2]$	+4.065(26)	+3.065	+2.989
$\mu(\frac{3}{2}_1^{\pm}\frac{1}{2}) [\mu_N]$	+2.689	+2.063	+2.597
$rms(\text{Exp} - \text{Th}) [\text{MeV}]$	-	1.067	1.765
$B(\text{E2};\frac{3}{2}_1^{\pm}\frac{1}{2} \rightarrow \frac{1}{2}_1^{\pm}\frac{1}{2})$	2.6(4)	1.476	0.750
$B(\text{GT};\frac{3}{2}_1^{\pm}\frac{1}{2} \rightarrow \frac{3}{2}_1^{\pm}\frac{1}{2})$	0.345(8)	0.235	0.663
$B(\text{GT};\frac{3}{2}_1^{\pm}\frac{1}{2} \rightarrow \frac{1}{2}_1^{\pm}\frac{1}{2})$	0.440(22)	0.461	0.841
$B(\text{GT};\frac{3}{2}_1^{\pm}\frac{1}{2} \rightarrow \frac{5}{2}_1^{\pm}\frac{1}{2})$	0.526(27)	0.526	0.394
$B(\text{GT};\frac{3}{2}_1^{\pm}\frac{1}{2} \rightarrow \frac{3}{2}_2^{\pm}\frac{1}{2})$	0.525(27)	0.762	0.574
$B(\text{GT};\frac{3}{2}_1^{\pm}\frac{1}{2} \rightarrow \frac{5}{2}_2^{\pm}\frac{1}{2})$	0.461(23)	0.829	0.236
${}^{12}\text{C} : E(0_1^{\pm}0) [\text{MeV}]$	92.162	95.57	84.76
$r_p [\text{fm}]$	2.35(2)	2.172	2.229
$Q(2_1^{\pm}0) [e \text{ fm}^2]$	+6(3)	+4.318	+4.931
$rms(\text{Exp} - \text{Th}) [\text{MeV}]$	-	1.058	1.318
$B(\text{E2};2_1^{\pm}0 \rightarrow 0_1^{\pm}0)$	7.59(42)	4.252	5.483
$B(\text{M1};1_1^{\pm}0 \rightarrow 0_1^{\pm}0)$	0.0145(21)	0.006	0.003
$B(\text{M1};1_1^{\pm}1 \rightarrow 0_1^{\pm}0)$	0.951(20)	0.913	0.353
$B(\text{E2};2_1^{\pm}1 \rightarrow 0_1^{\pm}0)$	0.65(13)	0.451	0.301
${}^{13}\text{C} : E(\frac{1}{2}_1^{\pm}\frac{1}{2}) [\text{MeV}]$	97.108	103.23	90.31
$r_p(\frac{1}{2}_1^{\pm}\frac{1}{2}) [\text{fm}]$	2.29(3)	2.135	2.195
$\mu(\frac{1}{2}_1^{\pm}\frac{1}{2}) [\mu_N]$	+0.702	+0.394	+0.862
$rms(\text{Exp} - \text{Th}) [\text{MeV}]$	-	2.144	2.089
$B(\text{E2};\frac{3}{2}_1^{\pm}\frac{1}{2} \rightarrow \frac{1}{2}_1^{\pm}\frac{1}{2})$	6.4(15)	2.659	4.584
$B(\text{M1};\frac{3}{2}_1^{\pm}\frac{1}{2} \rightarrow \frac{1}{2}_1^{\pm}\frac{1}{2})$	0.70(7)	0.702	1.148
$B(\text{GT};\frac{1}{2}_1^{\pm}\frac{1}{2} \rightarrow \frac{1}{2}_1^{\pm}\frac{1}{2})$	0.20(2)	0.095	0.328
$B(\text{GT};\frac{1}{2}_1^{\pm}\frac{1}{2} \rightarrow \frac{3}{2}_1^{\pm}\frac{1}{2})$	1.06(8)	1.503	2.155
$B(\text{GT};\frac{1}{2}_1^{\pm}\frac{1}{2} \rightarrow \frac{1}{2}_2^{\pm}\frac{1}{2})$	0.16(1)	0.733	0.263
$B(\text{GT};\frac{1}{2}_1^{\pm}\frac{1}{2} \rightarrow \frac{3}{2}_2^{\pm}\frac{1}{2})$	0.39(3)	1.050	0.221
$B(\text{GT};\frac{1}{2}_1^{\pm}\frac{1}{2} \rightarrow \frac{3}{2}_1^{\pm}\frac{3}{2})$	0.19(2)	0.400	0.151
Total energy rms [MeV]	-	1.314	1.671

what uncertain (see e.g. Ref. [12]), it will be important to study the sensitivity of our results with respect to this strength. Further on, it will be interesting to incorporate sub-leading NNN interactions and also four-nucleon interactions, which are also order $N^3\text{LO}$ [22]. Finally, we plan to extend the basis spaces to $N_{\max} = 8$ ($8\hbar\Omega$) for $A > 6$ to further improve convergence.

Our overall conclusion is that these results provide major impetus for the full program of deriving the nucleon-nucleon interaction and its multi-nucleon partners in the consistent approach provided by chiral effective field theory. It is straightforward, but challenging, to extend this research thrust in the directions indicated. The favorable results to date and the need for addressing fundamental symmetries of strongly interacting systems with enhanced predictive power, firmly motivates this path.

This work was partly performed under the auspices of the U. S. Department of Energy by the University of California, Lawrence Livermore National Laboratory under contract No. W-7405-Eng-48. Support from the LDRD contract No. 04-ERD-058 and from U.S. DOE/SC/NP (Work Proposal No. SCW0498) and from the U. S. Department of Energy Grant DE-FG02-87ER40371 is acknowledged. Numerical calculations have been performed at the LLNL LC and at the NERSC facilities, Berkely, and at the NIC, Jülich.

[1] S. Weinberg, Physica **96A**, 327 (1979); Phys. Lett. B **251**, 288 (1990); Nucl. Phys. **B363**, 3 (1991); J. Gasser *et al.*, Ann. of Phys. **158**, 142 (1984).

[2] V. Bernard *et al.*, Int. J. Mod. Phys. E4, 193 (1995).

[3] C. Ordonez *et al.*, Phys. Rev. Lett. **72**, 1982 (1994).

[4] U. van Kolck, Prog. Part. Nucl. Phys. **43**, 337 (1999).

[5] P. F. Bedaque and U. van Kolck, Ann. Rev. Nucl. Part. Sci. **52**, 339 (2002); E. Epelbaum, Prog. Part. Nucl. Phys. **57**, 654 (2006).

[6] S. R. Beane *et al.*, Phys. Rev. Lett. **97**, 012001 (2006).

[7] D. R. Entem *et al.*, Phys. Rev. C **68**, 041001(R) (2003).

[8] U. van Kolck, Phys. Rev. C **49**, 2932 (1994); E. Epelbaum *et al.*, Phys. Rev. C **66**, 064001 (2002).

[9] P. Navrátil, J. P. Vary and B. R. Barrett, Phys. Rev. Lett. **84**, 5728 (2000); Phys. Rev. C **62**, 054311 (2000).

[10] P. Navrátil *et al.*, Phys. Rev. Lett. **88**, 152502 (2002).

[11] P. Navrátil *et al.*, Phys. Rev. C **68**, 034305 (2003).

[12] A. Nogga *et al.*, Phys. Rev. C **73**, 064002 (2006).

[13] A. C. Hayes *et al.*, Phys. Rev. Lett. **91**, 012502 (2003).

[14] F. Ajzenberg-Selove, Nucl. Phys. **A490**, 1 (1988).

[15] F. Ajzenberg-Selove, Nucl. Phys. **A506**, 1 (1990).

[16] F. Ajzenberg-Selove, Nucl. Phys. **A523**, 1 (1991).

[17] I. Tanihata *et al.*, Phys. Lett. B **206**, 592 (1988).

[18] A. Ozawa *et al.*, Nucl. Phys. **A608**, 63 (1996); H. De Vries, C. W. De Jager, and C. De Vries, At. Data Nucl. Data Tables **36**, 495 (1987).

[19] I. Daito *et al.*, Phys. Lett. B **418**, 27 (1998).

[20] Y. Fujita *et al.*, Phys. Rev. C **70**, 011306(R) (2004).

[21] X. Wang *et al.*, Phys. Rev. C **63**, 024608 (2001).

[22] E. Epelbaum, Phys. Lett. B **639**, 456 (2006).